

# Catalytic Amplification of Patterning via Surface-Confined Ring-Opening Metathesis Polymerization on Mixed Primer Layers Formed by Contact Printing

Yoshiko Harada, Gregory S. Girolami,\* and Ralph G. Nuzzo\*,†

Department of Chemistry and the Frederick Seitz Materials Research Laboratory,  
University of Illinois at Urbana–Champaign, Urbana, Illinois 61801

Received November 20, 2002. In Final Form: March 14, 2003

Thin films of polymers synthesized from strained olefins were formed on Si(100) via ring-opening metathesis polymerization (ROMP) initiated by a Ru–alkylidene catalyst bound to the surface by means of the alkylidene ligands. Specifically, a mixture of 7-octenyltrichlorosilane (**3**) and octyltrichlorosilane (**4**) was deposited onto Si/SiO<sub>2</sub> surfaces via contact printing, and this assembly was subsequently treated with RuCl<sub>2</sub>(PCy<sub>3</sub>)<sub>2</sub>(=CHPh) (**1**). The resulting surface-tethered Ru alkylidene complex reacts with norbornene derivatives to give thin polymer films. The growth of the polymer film, as monitored by ellipsometry, X-ray photoelectron spectroscopy (XPS), and atomic force microscopy (AFM), is strongly influenced by the initial concentration of the catalyst at the surface and by the monomer reactivity. The catalyst concentration at the Si/SiO<sub>2</sub> surface was controlled by adjusting the relative ratio of **3** and **4** in the “primer” used in the contact-printing step. These studies revealed that the success of the catalytic amplification step required that the linker be present on the surface in very low coverage. The optimal concentration of **3** in the mixed primer was 20–40% with a total mass coverage of the mixed self-assembled monolayer (SAM) of approximately one-third that of a full monolayer coverage. Possible causes of the inefficient polymerization at high coverages of **3** are discussed; a leading candidate is that the catalytic Ru centers are deactivated by reactions with neighboring olefinic linker sites or with other Ru centers. In a representative class of polymerization, reticulated films of poly(2,2,2-trifluoroethyl bicyclo[2.2.1]hept-2-ene-5-carboxylate) (**5**) with an average thickness of ~100 Å were obtained after ~3 h of reaction at room temperature. The polymerization can be completely described by a rate law involving coupled step-growth and competing unimolecular termination reactions. The polymerization process can be used to amplify catalytically (that is, to increase the mass coverages of) latent images present in SAMs that have been patterned via microcontact printing ( $\mu$ CP). To do so, a patterned resist SAM of octadecyltrichlorosilane (OTS) was deposited first via  $\mu$ CP. A second SAM based on the mixed phase of **3** and **4** was then orthogonally assembled in a self-registering printing step carried out using an unpatterned poly(dimethylsiloxane) (PDMS) stamp. Activation of this composite SAM via a treatment first with **1** and then with **5** resulted in an additive deposition of the polymer pattern.

## Introduction

The deposition of polymer films onto solid substrates such as Si wafers and glass is a key step in the fabrication of integrated systems for cell engineering,<sup>1,2</sup> optoelectronics,<sup>3–5</sup> sensors,<sup>6–10</sup> and micromachines.<sup>11</sup> Several methods for obtaining polymer films on solid substrates have been developed, of which polymerization by means

of a surface-anchored reagent has received increasing attention. Surface-initiated polymerization is useful for producing covalently bound, dense, thick polymer layers, ones that are difficult to obtain by more traditional methods such as the “grafting to” technique.<sup>12–15</sup> In the “grafting to” method, preformed polymer chains are directly adsorbed on the surface, but complete coverage of the surface is difficult to achieve because grafting of polymer chains becomes increasingly more difficult with time, as more macromolecules occupy and hinder the remaining surface sites. In contrast, surface-initiated polymerization—in which a polymer is formed from a solution of the monomer by action of a surface-bound initiator—can provide better control over the graft density.<sup>12–15</sup>

Examples of surface-initiated polymerization on substrates such as Au and Si/SiO<sub>2</sub> by free radical polymerization,<sup>12,13,16–19</sup> atom transfer radical polymerization

† Telephone: 217-244-0809. Fax: 217-244-2278. E-mail: r-nuzzo@uiuc.edu.

(1) Lu, L.; Yaszemski, M. J.; Mikos, A. G. *Biomaterials* **2001**, *22*, 3345–3355.

(2) Ostuni, E.; Chen, C. S.; Ingber, D. E.; Whitesides, G. M. *Langmuir* **2001**, *17*, 2828–2834.

(3) Sirringhaus, H.; Tessler, N.; Friend, R. H. *Science* **1998**, *280*, 1741–1744.

(4) Dodabalapur, A.; Bao, Z.; Makhija, A.; Laquindanum, J. G.; Raju, V. R.; Feng, Y.; Katz, H. E.; Rogers, J. A. *Appl. Phys. Lett.* **1998**, *73*, 142–144.

(5) Kim, E.; Whitesides, G. M.; Lee, L. K.; Smith, S. P.; Prentiss, M. *Adv. Mater.* **1996**, *8*, 139–142.

(6) Yang, J.; Swager, T. M. *J. Am. Chem. Soc.* **1998**, *120*, 11864–11873.

(7) Bubb, D. M.; McGill, R. A.; Horwitz, J. S.; Fitz-Gerald, J. M.; Houser, E. J.; Wu, P. W.; Ringelsen, B. R.; Piqué, A.; Chrisey, D. B. *J. Appl. Phys.* **2001**, *89*, 5739–5746.

(8) Kim, J.; McQuade, D. T.; McHugh, S. K.; Swager, T. M. *Angew. Chem., Int. Ed. Engl.* **2000**, *39*, 3868–3872.

(9) Liu, Y.; Zhao, M.; Bergbreiter, D. E.; Crooks, R. M. *J. Am. Chem. Soc.* **1997**, *119*, 8720–8721.

(10) Ito, Y.; Park, Y. S.; Imanishi, Y. *J. Am. Chem. Soc.* **1997**, *119*, 2739–2740.

(11) Jager, E. W. H.; Smela, W.; Inganäs, O. *Science* **2000**, *290*, 1540–1545.

(12) Prucker, O.; Rühle, J. *Langmuir* **1998**, *31*, 592–601.

(13) Prucker, O.; Rühle, J. *Macromolecules* **1998**, *31*, 602–613.

(14) Jordan, R.; Ulman, A.; Kang, J. F.; Raffailovich, M. H.; Sokolov, J. *J. Am. Chem. Soc.* **1999**, *121*, 1016–1022.

(15) Jordan, R.; Ulman, A. *J. Am. Chem. Soc.* **1998**, *120*, 243–247.

(16) Prucker, O.; Rühle, J. *Langmuir* **1998**, *14*, 6893–6898.

(17) Husemann, M.; Malmström, E. E.; McNamara, M.; Mate, M.; Mecerreyes, D.; Benoit, D. G.; Hendrick, J. L.; Mansky, P.; Huan, E.; Russell, T. P.; Hawker, C. J. *Macromolecules* **1999**, *32*, 1424–1431.

(18) Hyun, J.; Chilkoti, A. *Macromolecules* **2001**, *34*, 5644–5652.

(19) Huang, W.; Ganesan, S.; Baker, G. L.; Bruening, M. L. *Langmuir* **2001**, *17*, 1731–1736.

(ATRP),<sup>17,19–27</sup> cationic<sup>15,28</sup> and anionic<sup>14,29,30</sup> polymerization, and ring-opening polymerization<sup>31–38</sup> have been reported. Both cationic and anionic polymerization methods have been used to synthesize surface-bound polymer brushes, but the procedures are long and, in particular, the sensitivity of anionic polymerization to impurities limits the utility of this process for polymerization onto solid substrates. Free radical polymerization has been employed successfully to grow >100 Å thick polystyrene films on flat substrates within 12 h.<sup>16</sup> The elevated temperatures required for free radical polymerization reactions, however, are incompatible with some chemical systems such as Au substrates modified with alkanethiol derivatives.<sup>19</sup> Surface polymerization by ATRP is very promising: film growth is well-controlled, and a wide variety of monomers can be used. For example, living polymerization by ATRP can afford >100 Å thick poly(methyl methacrylate) films. By combining cationic polymerization and ATRP, block copolymer films of styrene and methyl methacrylate have been prepared.<sup>39</sup> Use of mixed monolayers to initiate polymerization by ATRP has also been demonstrated.<sup>21</sup> Although many of the earlier ATRP procedures used unbound initiator or other reagents with similar functions to compensate for the low concentration of the surface-bound initiators, milder conditions requiring no “free” initiator have now been developed.<sup>20,21,25</sup> These newer methods have improved the performance of the process by eliminating the need for extensive washing to remove unbound polymer.

In this work, we studied ring-opening metathesis polymerization (ROMP) catalyzed by a surface-bound derivative of Grubbs' Ru compound, RuCl<sub>2</sub>(PCy<sub>3</sub>)<sub>2</sub>(=CHPh) (**1**).<sup>40</sup> This compound has been used in surface-initiated polymerization studies on both Au<sup>36</sup> and Si<sup>37,38,41</sup> substrates. In ROMP, the catalyst remains bonded to the

growing end of the polymer chain as the olefin monomer is repeatedly inserted into the chain. In the method described by Weck et al.,<sup>36</sup> a Au surface was first coated with a dodecanethiol self-assembled monolayer (SAM),<sup>42,43</sup> followed by insertion<sup>44</sup> of anchoring molecules bearing a terminal olefin group, at the domain boundaries of the dodecanethiol SAM. Grubbs' Ru catalyst was subsequently attached to the olefin linker, and strained olefin monomers were polymerized to give polymer patches grown from the domain boundaries defined by the initial alkanethiol SAM. Because polymerization was designed to take place at the structural domain boundaries only, this procedure resulted in an inhomogeneous polymer coating of low overall coverage. In an alternative approach, uniform polymer films of norbornene and its derivatives have been obtained by affixing **1** to a Si wafer derivatized with 5-(bicycloheptenyl)trichlorosilane (**2**).<sup>37,41</sup> The main drawback in this procedure is that the anchoring molecule, **2**, is not an ideal material for self-assembly. This Lewis acid sensitive compound must be handled with care so that the cycloolefin functionality is not altered by side reactions in the self-assembly<sup>45–47</sup> step. Self-assembly of **2** by contact printing has been attempted, but the film formation process was too slow for the method to be practical.<sup>41</sup>

In the present study, we have chosen a linear alkenylsilane, 7-octenyltrichlorosilane (**3**), as the anchoring molecule. The terminal olefin group of this molecule can undergo metathesis with the benzyldiene group of **1** to form a catalytically active layer. The use of terminal olefin groups in surface-confined ROMP has been demonstrated on Si(111)<sup>38</sup> and a polymeric substrate.<sup>35</sup> Because **3** is not a cyclic olefin, it is less susceptible to side reactions and, like its analogues such as octadecyltrichlorosilane (OTS), it can be deposited by either immersion or contact printing. Contact printing<sup>48,49</sup> is significantly more efficient than immersion, and it can be used to form surface patterns and to create multilayered structures by orthogonal self-assembly.<sup>50,51</sup> The studies reported here demonstrate that the surface density of the linker **3** has a significant impact on the number of catalytically active Ru sites that can be attached to the surface. By using inks consisting of mixtures of **3** with inactive species (octyltrichlorosilane, **4**), we were able to enhance the concentration of the catalyst bound to the primer layer in an active form. In this report, we show that surface-initiated ROMP of strained olefins is dramatically affected by both the catalyst loading and the reactivity of the monomer. This work complements earlier work on surface-initiated ROMP, and affords new insight into the surface polym-

- (20) Jones, D. M.; Huck, T. S. W. *Adv. Mater.* **2001**, *13*, 1256–1259.
- (21) Jones, D. M.; Brown, A. A.; Huck, T. S. W. *Langmuir* **2002**, *18*, 1265–1269.
- (22) Yamamoto, S.; Ejaz, M.; Tsujii, Y.; Fukuda, T. *Macromolecules* **2000**, *33*, 5608–5612.
- (23) Ejaz, M.; Yamamoto, S.; Ohno, K.; Tsuji, Y.; Fukuda, T. *Macromolecules* **1998**, *31*, 5934–5936.
- (24) Huang, X.; Doneski, L. J.; Wirth, M. J. *Anal. Chem.* **1998**, *70*, 4023–4029.
- (25) Kim, J.-B.; Bruening, M. L.; Baker, G. L. *J. Am. Chem. Soc.* **2000**, *122*, 7616–7617.
- (26) Matyjaszewski, K.; Miller, P. J.; Shukla, N.; Immaraporn, B.; Gelman, A.; Luokkala, B. B.; Siclován, T. M.; Kickelbick, G.; Vallant, T.; Hoffmann, H.; Pakula, T. *Macromolecules* **1999**, *32*, 8716–8724.
- (27) Shah, R. R.; Merceyeyes, D.; Husemann, M.; Rees, I.; Abbott, N. L.; Hawker, C. J.; Hedrick, J. L. *Macromolecules* **2000**, *33*, 597–605.
- (28) Jordan, R.; West, N.; Ulman, A.; Chou, Y.-M.; Nuyken, O. *Macromolecules* **2001**, *34*, 1606–1611.
- (29) Oosterling, M. L. C. M.; Sein, A.; Schouten, A. J. *Polymer* **1992**, *33*, 4394–4400.
- (30) Ingall, M. D. K.; Honeyman, C. H.; Mercure, J. V.; Bianconi, P. A.; Kunz, R. R. *J. Am. Chem. Soc.* **1999**, *121*, 3607–3613.
- (31) Husemann, M.; Mecerreyes, D.; Hawker, C. J.; Hedrick, J. L.; Shah, R.; Abbott, N. L. *Angew. Chem., Int. Ed. Engl.* **1999**, *38*, 647–649.
- (32) Heise, A.; Menzel, H.; Yim, H.; Foster, M. D.; Wieringa, R. H.; Schouten, A. J.; Erb, V.; Stamm, M. *Langmuir* **1997**, *13*, 723–728.
- (33) Wieringa, R. H.; Schouten, A. J. *Macromolecules* **1996**, *29*, 3032–3034.
- (34) Buchmeiser, M. R.; Sinner, F.; Mupa, M.; Wurst, K. *Macromolecules* **2000**, *33*, 32–29.
- (35) Preishuber-Pflügl, P.; Podolan, R.; Stelzer, F. *J. Mol. Catal. A: Chem.* **2000**, *160*, 53–61.
- (36) Weck, M.; Jackiw, J. J.; Rossi, R. R.; Weiss, P. S.; Grubbs, R. H. *J. Am. Chem. Soc.* **1999**, *121*, 4088–4089.
- (37) Kim, N. Y.; Jeon, N. L.; Choi, I. S.; Takami, S.; Harada, Y.; Finnie, K. R.; Girolami, G. S.; Nuzzo, R. G.; Whitesides, G. M.; Laibinis, P. E. *Macromolecules* **2000**, *33*, 2793–2795.
- (38) Juang, A.; Scherman, O. A.; Grubbs, R. H.; Lewis, N. S. *Langmuir* **2001**, *17*, 1321–1323.
- (39) Zhao, B.; Brittain, W. J. *J. Am. Chem. Soc.* **1999**, *121*, 3557–3558.
- (40) Schwab, P.; Grubbs, R. H.; Ziller, J. W. *J. Am. Chem. Soc.* **1996**, *118*, 100–110.

- (41) Jeon, N. L.; Choi, I. S.; Whitesides, G. M.; Kim, N. Y.; Laibinis, P. E.; Harada, Y.; Finnie, K. R.; Girolami, G. S.; Nuzzo, R. G. *Appl. Phys. Lett.* **1999**, *75*, 4201–4203.
- (42) Ulman, A. *Chem. Rev.* **1996**, *96*, 1544–1554.
- (43) Ulman, A. *An introduction to ultrathin organic films: from Langmuir–Blodgett to self-assembly*; Academic Press: Boston, MA, 1991.
- (44) Cygan, M. T.; Dunbar, T. D.; Arnold, J. J.; Bumm, L. A.; Shdlock, N. F.; Burgin, T. P.; Jones, L. I.; Allara, D. L.; Tour, J. M.; Weiss, P. S. *J. Am. Chem. Soc.* **1998**, *120*, 2721–2732.
- (45) Lehn, J. M. *Angew. Chem., Int. Ed. Engl.* **1988**, *27*, 89–112.
- (46) Philp, D.; Stoddart, J. F. *Angew. Chem., Int. Ed. Engl.* **1996**, *35*, 1154–1196.
- (47) Whitesides, G. M.; Mathias, J. P.; Seto, C. T. *Science* **1991**, *254*, 1312–1319.
- (48) Xia, Y.; Whitesides, G. M. *Angew. Chem., Int. Ed. Engl.* **1998**, *37*, 550–575.
- (49) Michel, B.; Bernard, A.; Bietsch, A.; Delamarche, E.; Geissler, M.; Juncker, D.; Kind, H.; Renault, J. P.; Rothuizen, H.; Schmid, H.; Schmidt-Winkel, P.; Stutz, R.; Wolf, H. *IBM J. Res. Dev.* **2001**, *45*, 697–719.
- (50) Hickman, J. J.; Laibinis, P. E.; Auerbach, D. I.; Zou, C.; Gardner, T. J.; Whitesides, G. M.; Wrighton, M. S. *Langmuir* **1992**, *8*, 357–359.
- (51) Laibinis, P. E.; Hickman, J. J.; Wrighton, M. S.; Whitesides, G. M. *Science* **1989**, *245*, 845–847.

erization process occurring with this immobilized catalyst system.

### Experimental Section

**Materials.** Octadecyltrichlorosilane (Aldrich), 7-octenyltrichlorosilane (Gelest), octyltrichlorosilane (Gelest), and 5-(bicycloheptenyl)trichlorosilane (Gelest) were vacuum distilled and stored under nitrogen in a glovebox. 1,2-Dichloroethane (Fisher) was dried with  $\text{CaCl}_2$ , distilled over  $\text{CaSO}_4$  under Ar, sparged with Ar, and stored in a glovebox. 2-Propanol (Fisher), toluene (Fisher), norbornene (Aldrich), 2,2,2-trifluoroethyl acrylate (Aldrich), and  $\text{RuCl}_2(\text{PCy}_3)_2(=\text{CHPh})$  (Strem) were used as received. Norbornadiene was distilled over activated alumina under Ar, and stored in a glovebox. Dichloromethane was dried with  $\text{CaH}_2$  and distilled under  $\text{N}_2$ . Water was deionized and purified using a custom built system meeting clean room specifications for particulates and residual conductivity.

**2,2,2-Trifluoroethyl bicyclo[2.2.1]-hept-2-ene-5-carboxylate (5).** To a  $\text{CH}_2\text{Cl}_2$  (75 mL) solution of freshly distilled cyclopentadiene (6.25 g, 94.5 mmol) was added 2,2,2-trifluoroethyl acrylate (3.00 mL, 23.7 mmol) slowly at  $0^\circ\text{C}$  under Ar. The solution was stirred and allowed to warm to room-temperature overnight. The solvent was removed under vacuum, and the remaining product was distilled under vacuum. A clear liquid (5.13 g, 98% yield) was obtained. The endo and exo isomers were not separated.

**Surface-Initiated Polymerization.** Toluene solutions of the silanes were prepared in a nitrogen-filled glovebox immediately before use. For the formation of mixed monolayers of 7-octenyltrichlorosilane (**3**) and octyltrichlorosilane (**4**), 10 mM solutions consisting of various mole fractions of each were used as inks in contact printing.

B-doped, p-type Si(100) wafers (Silicon Sense, test grade,  $1\text{--}25\ \Omega\ \text{cm}$ ) were cut into  $\sim 1 \times 1\ \text{cm}^2$  pieces and cleaned in piranha solution (3:1  $\text{H}_2\text{SO}_4\text{:H}_2\text{O}_2$ ) for 2 min, rinsed with deionized water (DI), and dried in a stream of nitrogen. The wafers were then placed in a UV/ozone chamber for at least 15 min, rinsed with DI, and dried with nitrogen.

Contact printing was performed with a poly(dimethylsiloxane) (PDMS) stamp coated with organosilane solutions using a photoresist spinner (3000 rpm for 30 s). The stamp was dried for 30 s in a nitrogen stream and was manually placed on a clean silicon substrate. The substrate was held at a constant temperature on a hot plate, or it was handled at room temperature. Contact printed wafers were rinsed with 2-propanol (IPA) and DI, and were dried in a stream of nitrogen. For orthogonal self-assembly of OTS and mixtures of **3** and **4**, the substrate was patterned by  $\mu\text{CP}$  with an OTS pattern, rinsed and dried, and then contact printed with an unpatterned PDMS stamp inked with a solution containing **3** and **4**. Because the trichlorosilane reagents are sensitive to the water content and temperature of the printing ambient, the relative humidity and the temperature of the room were monitored by a thermohygrometer (Fisher). The dew point (typically  $\sim 10^\circ\text{C}$  for high humidity and  $\sim 2^\circ\text{C}$  for low humidity conditions) was lower than the reaction temperature ( $\sim 22\text{--}24^\circ\text{C}$ ) for all experiments.

In a nitrogen-filled glovebox, the samples were immersed in a 10 mM 1,2-dichloroethane (DCE) solution of the Ru catalyst for 30 min at room temperature. The samples were rinsed thoroughly with DCE, and immersed in monomer solutions at room temperature. The samples were removed from the monomer solutions and rinsed with DCE, and dried in a stream of nitrogen. After the samples were transferred out of the glovebox, they were rinsed with IPA and DI, and dried with nitrogen.

**Instrumental Methods.** Ellipsometry measurements were recorded using a Gaertner Scientific (model L116C) ellipsometer equipped with a He-Ne laser (6328 Å), set at an angle of incidence of  $70^\circ$ . The substrate constants were derived from ellipsometric measurements conducted at eight or more locations on an uncoated substrate. For coated substrates, the thickness of the deposited film was determined from ellipsometric measurements at 5–10 spots, using the recorded substrate constants and assuming that the refractive index of the film was 1.5.<sup>52</sup> Atomic force microscopy (AFM) images were collected on a Digital Instruments Dimension 3100 scanning probe microscope. Height contrast images were recorded with a silicon probe in the tapping

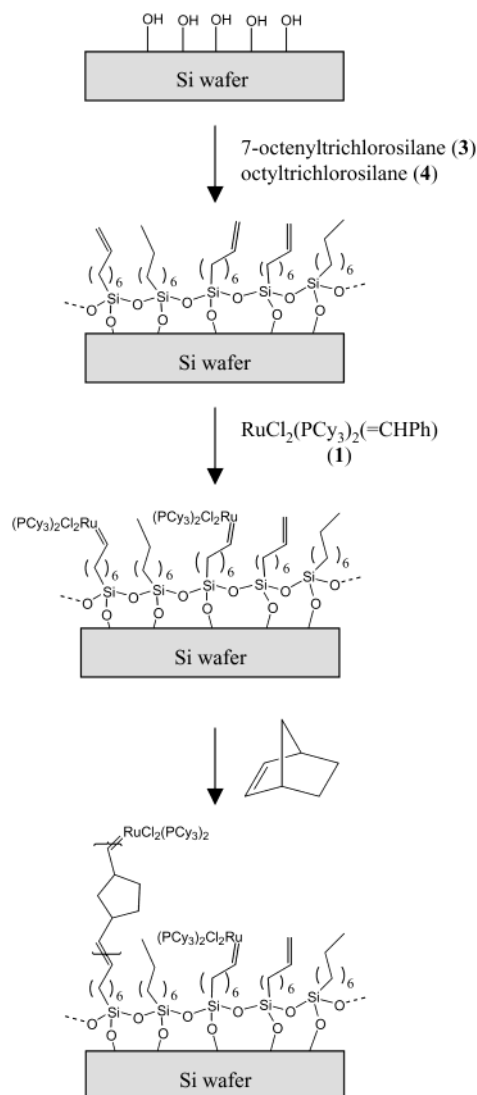


**Figure 1.** Procedure used to form a polymer film on a Si substrate. An ink composed of **3** and **4** is contact printed on a silicon wafer. The functionalized wafer is then immersed in a 10 mM solution of **1** and rinsed with DCE. Finally, the substrate is immersed in a monomer solution (norbornene in this figure) to form a polymer film by ROMP.

mode, applying a minimum force to maintain the necessary feedback. The chemical compositions of all the films except for the Ru-coated sample in Figure 5 and the poly(norbornene) film (Supporting Information) were analyzed by X-ray photoelectron spectroscopy (XPS) on a Kratos AXIS ULTRA spectrometer. Survey scans were collected with a monochromatic Al K $\alpha$  source (15 kV, 225 W) at a constant pass energy of 160 eV. Multiplex scans were collected at a pass energy of 20 eV. XPS images were acquired in the parallel imaging mode at a constant pass energy of 160 eV with the minimum iris size of  $\sim 2.5\ \text{mm}$ . Fluorine maps were obtained at 687 eV, and were corrected for charging and background noise. All samples were analyzed at a  $90^\circ$  angle relative to the sample surface with the neutralizer on. The surface chemical compositions of the Ru-coated sample and the poly(norbornene) sample were determined on a Physical Electronics PHI 5400 spectrometer using a monochromatic Al K $\alpha$  source (15 kV, 500 W). The survey scans were collected at a constant pass energy of 178.95 eV at a  $45^\circ$  tilt angle.

### Results and Discussion

The overall procedure used to grow unpatterned polymer films on  $\text{Si/SiO}_2$  by ROMP is summarized in Figure 1.



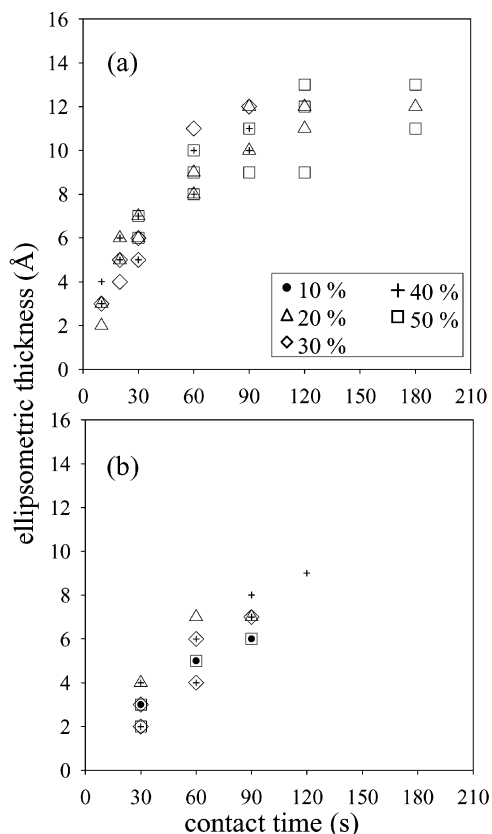


**Figure 2.** Growth via contact printing of mixed monolayers of the silanes **3** and **4** as monitored by ellipsometry. The composition of the ink is shown as the fraction of **3** in the ink. The films were prepared by contact printing at room temperature ( $\sim 22$ – $24$  °C) under (a) high relative humidity (dew point  $\sim 10$  °C), and (b) low relative humidity (dew point  $\sim 2$  °C) conditions.

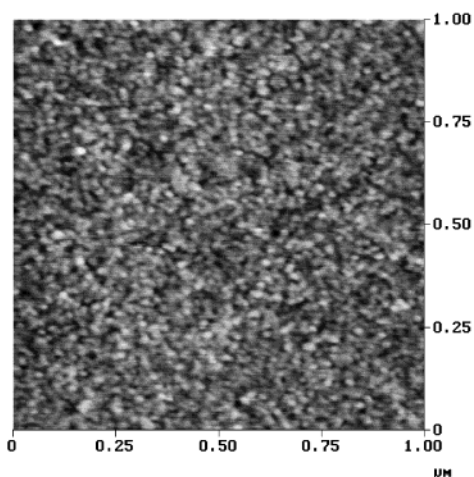


**Figure 3.**  $1\ \mu\text{m} \times 1\ \mu\text{m}$  AFM image of the primer layer formed by contact printing a 10 mM solution of 40% **3** for 30 s. The ellipsometric thickness of the film was  $\sim 4$  Å ( $\theta \approx 0.3\theta_{\text{sat}}$ ).

First, a Si wafer was contact printed with a 10 mM solution composed of a mixture of 7-octenyltrichlorosilane (**3**) and octyltrichlorosilane (**4**) in toluene under ambient conditions, using a featureless (flat) PDMS stamp. The primed wafer was then transferred into a nitrogen-filled glovebox, where it was immersed in a 10 mM solution of  $\text{RuCl}_2(\text{PCy}_3)_2(=\text{CHPh})$  (**1**) in 1,2-dichloroethane (DCE) for 30 min at room temperature. The Ru catalyst reacts with the alkene functional group of **3** by metathesis. Polymer films were then grown on the surface by immersing the

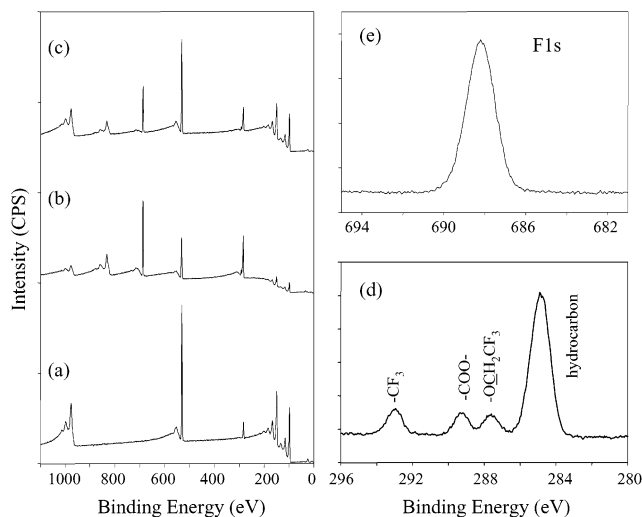


**Figure 4.** XPS survey scans of (a) a 40% **3** primer layer, (b) a  $\sim 55$  Å film prepared by ROMP on 40% **3** (F/Si  $\sim 73/27$ ), and (c) a  $\sim 13$  Å film prepared by ROMP on 100% **3** (F/Si  $\sim 30/70$ ). All survey spectra are normalized to the same intensity scale. XPS multiplex scans of (d) C 1s, and (e) F 1s core levels, recorded using the sample in part b. Polymerization was carried out for 1 h at room temperature using 0.2 M **5**.

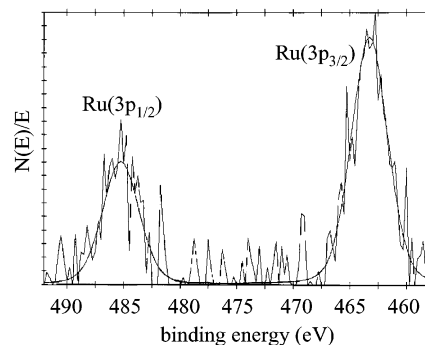


**Figure 5.** X-ray photoelectron spectrum of Ru 3p core level peaks acquired from a sample bearing a monolayer of **3** supported on a Si(100) substrate following treatment with the Ru catalyst.

sample in a solution of a norbornene monomer in DCE for a set amount of time, usually between 10 min and 4 h, at room temperature. Each step in the procedure was characterized ex situ using quenched samples.

It is worth commenting on our choice of monomer, 2,2,2-trifluoroethyl bicyclo[2.2.1]hept-2-ene-5-carboxylate (**5**). We selected this monomer in part because its rate of polymerization by ROMP is slow, thus allowing the polymerization process to be monitored conveniently in an ex situ fashion by ellipsometry, XPS, and AFM. In contrast, norbornene (a monomer we have used in the past) is very reactive in surface-initiated ROMP<sup>37,38,41</sup> and, as a result, it is difficult to observe the initial polymer growth process even at low monomer concentrations ( $\leq 5$  mM). We found, for example, that exposure of the catalyst-loaded surface to a 0.1 M solution of norbornene in DCE rapidly deposited polymer films with thicknesses as high as  $\sim 800$ – $900$  Å. The Supporting Information shows an XPS spectrum of one representative film grown in this way, one notable for its complete attenuation of the Si(100) substrate core levels. Polymerization of norbornene derivatives with a substituent in the 5-position is not as rapid but is still facile by surface-initiated ROMP.<sup>37,41</sup> Monomers such as 5-(bicycloheptenyl)trichlorosilane (**2**) and 5-(bicycloheptenyl)triethoxysilane are poor choices because they have functional groups that may undergo

hydrolysis and complicate the reaction mechanism; the monomer we chose for the kinetic study, **5**, has no such functional groups and (as we show) is well behaved kinetically (see below). Finally, the presence of fluorine atoms in **5** allows the progress of the polymerization to be followed conveniently by monitoring the F(1s) signal in the XPS spectrum.

The effect of the composition of the primer layer on polymerization was studied by changing the surface concentration of the catalyst anchoring group, 7-octenyl-trichlorosilane (**3**). This study was prompted by the unexpected finding that dense monolayers of pure **3** were inefficient as primers for the Ru-catalyzed polymerization of norbornenes, but that low coverages of **3** were much more effective (see below). To vary the surface concentration of **3** in a systematic way, mixed primer layers were formed by inking the surface with a mixture of **3** and the olefin-free monomer octyltrichlorosilane (**4**). Because the two components are similar in structure, we expected them to bond similarly to the substrate and mix uniformly rather than segregate into domains containing only one of the components. Although the exact composition of the contact printed films on the substrate is unknown, we refer to them by the mole fraction of **3** used to formulate the ink.

**Formation of Mixed Primer Layers by Contact Printing.** Mixed composition films of **3** and **4** were easily prepared by contact printing from a range of ink compositions (Figure 2). In the sections that follow, we show that the polymerizations mediated by the tethered ROMP catalyst are exceedingly sensitive to the ink composition and coverage. The best polymer films were obtained when the primer was prepared from inks that had low mole fractions of **3** or was prepared under printing conditions that transferred less than a full monolayer coverage of the silanes. For this reason, we developed experimental procedures that served to deliver such printed organosilane SAMs. The ellipsometric thickness of a typical primer film prepared by contact printing a 10 mM ink containing 40% **3** (mole fraction in a toluene solution of **3** and **4**) for 30 s, for example, was  $\sim 4$  Å. This thickness corresponds to  $\sim 1/3$  of the value expected for a full coverage of a mixed-SAM of the same composition. The measured, average thicknesses of pure films of **3** and **4** on Si/SiO<sub>2</sub> at full coverage are  $\sim 12.5$  and  $\sim 13.6$  Å, respectively.<sup>53</sup> The mass coverage of a complete mixed-SAM also falls in this range, as shown by the limiting thickness (Figure 2) of the contact printed layers grown from 10 mM inks containing various mole fractions of **3** and **4**.

Figure 2 also shows that the assembly rate of the mixed silane inks is impacted significantly by the water vapor pressure present in the printing environment, being faster under conditions of high relative humidity (a) than low relative humidity (b). This sensitivity has been examined and is discussed in more detail elsewhere.<sup>54</sup> We simply note here that layers with mass coverages well below a monolayer can be obtained (see below). Because the printing kinetics, and thus total surface coverages of these organosilanes, depend sensitively on the amount of water present in the reaction environment, we closely monitored the relative humidity and the temperature of the ambient. For the samples used in this work, the typical dew point was  $<6$  °C and room temperature was  $\sim 23$  °C. We found that, under such conditions, the contact printed primer films were largely free of multilayers or large cross-linked siloxane deposits for the 10 mM ink concentration used.

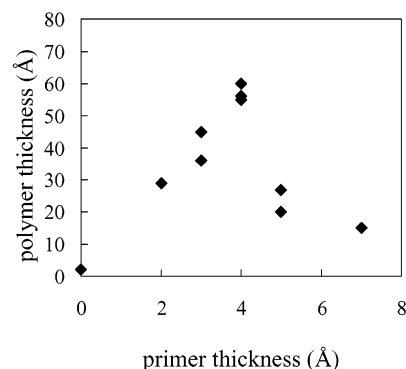


**Figure 6.** Ellipsometric thickness of polymer films after a 1 h reaction in a 0.2 M monomer solution of **5** prepared using a ROMP catalyst bound on a 40% **3** primer. The data show that the thickness of the resulting polymer film depends on the mass coverage of the primer layer.

AFM images (Figure 3) of the mixed monolayers reveal that the growth of the primer layer proceeds via the initial formation of granular domains that are  $\sim 200$  Å in size and randomly distributed across the surface. The example shown in Figure 3, taken at a representative mass coverage of approximately one-third of a full monolayer ( $\theta \approx 0.3\theta_{\text{sat}}$ ), shows that these domains are textured at the nanoscale. These domains do coarsen somewhat as the growth proceeds but never fully coalesce.

An XPS spectrum of a primer film contact printed for 30 s from an 10 mM ink consisting of 40 mol % **3** and 60 mol % **4** in toluene ( $\theta_{\text{tot}} \approx 0.3\theta_{\text{sat}}$ ) is shown in Figure 4a. The spectrum shows core level peaks characteristic of alkylsilane SAMs on Si/SiO<sub>2</sub>: O 1s at 532 eV, C 1s at 285 eV, Si 2s at 151 eV, and Si 2p at 99 eV. Ellipsometric data (see above) showed that the coverage of the organosilanes is small (submonolayer), and this conclusion is confirmed by the predominance of the peaks ascribed to the Si substrate (both elemental Si and silicon oxide) in the spectrum recorded from this sample.

**Attachment of the Ru Catalyst to Mixed Primer Layers.** We examined the attachment of the Ru catalyst to the printed SAM by XPS. In a representative experiment, a Si wafer coated with 100% **3** at full coverage was immersed in a 6 mM solution of **1** in DCE for 3 h under N<sub>2</sub>. The sample was then exhaustively rinsed with DCE and transferred to the UHV chamber. XPS analysis revealed Ru core level peaks at 485 eV (Ru 3p<sub>1/2</sub>) and at 463 eV (Ru 3p<sub>3/2</sub>), and the peak areas corresponded to a Ru/C ratio of less than 1% (Figure 5). The core level peaks in the Ru 3d region could not be examined due to the significant interferences that arise from overlapping C 1s core levels. The data are consistent with the presence of a low-valent Ru species, albeit one present at very low concentrations (see below).

**Surface-Initiated Ring-Opening Metathesis Polymerization on Mixed Primer Layers.** We conducted a variety of exploratory experiments to determine the optimal characteristics for a ROMP primer layer based on 7-octenyltrichlorosilane, **3**. Unexpectedly, films consisting solely of **3** (especially at high coverage) were poor primers: exposure to the Ru catalyst and then treatment with norbornene monomer **5** resulted in very little ROMP activity. Interestingly, priming the surface with an ink consisting of a mixture of **3** with the olefin-free octadecyltrichlorosilane **4** improved the catalytic efficiency, albeit in a way that still revealed significant sensitivity to the absolute mass coverage of the mixed SAM. The general trends we found are illustrated by the ellipsometry data shown in Figure 6, which show that optimal activity for

(53) Wasserman, S. R.; Tao, Y.-T.; Whitesides, G. M. *Langmuir* **1989**, 5, 1074–1087.

(54) Finnie, K. R.; Haasch, R.; Nuzzo, R. G. *Langmuir* **2000**, 16, 6968–6976.

a 40:60 **3**:**4** primer composition (which we adopt as a standard) was obtained at a total mass coverage of  $\theta_{\text{tot}} \approx 0.3\theta_{\text{sat}}$ . These data strongly suggest that the sites at which the Ru centers are anchored must be dilute, presumably to avoid reactions with neighboring linker sites or with Ru centers that deactivate the catalyst.

We then made direct comparisons of samples that were subjected to different initial treatments but otherwise identical procedures thereafter. One primer layer was generated from 40% **3**, whereas a second was prepared from 100% **3**. Both primer layers were printed to give a mass coverage of  $\sim 4$  Å; after the primed surfaces were treated with Ru catalyst **1** and exposed to monomer **5**, the ellipsometric thickness had increased by  $\sim 55$  and  $\sim 13$  Å, respectively. This result clearly shows that priming the surface with a mixture of **3** and **4** enhances the ROMP polymerization process. The difference noted by ellipsometry is reflected in the XPS spectra as well (Figure 4, parts b and c). Notably, the relative intensities of the F 1s and O 1s peaks are reversed in the two spectra, and the intensities of the Si 2s and Si 2p peaks are attenuated significantly in the mixed monolayer sample. Because the monomer **5** contains a carbonyl group, the oxygen peak is not expected to disappear completely, but the film grown from a primer layer consisting of 40% **3** had sufficient thickness to significantly attenuate the photoelectrons originating from the Si/SiO<sub>2</sub> substrate. Similar experiments conducted using mixed primer layers of  $\sim 11$  Å (close to full coverage) resulted in the maximum F/Si ratio when the fraction of **3** in the primer layer was in the 20–40% range. These data clearly support the observations made above and demonstrate that thicker polymer films are obtained by surface-initiated ROMP when the primer layer is printed from a mixture of **3** with a diluent, rather than pure **3** itself.

To verify that the polymerization activity observed was due to ROMP catalysis by surface-tethered Ru centers, blank experiments were carried out. A primed Si wafer and a bare Si wafer (neither of which had been treated with the Ru catalyst **1**) were immersed in a solution of monomer **5** for 1 h. Both samples showed negligible film growth by ellipsometry ( $<1$  Å) and XPS (no F 1s signal detected). When a bare Si wafer (not coated with primer) was immersed in a catalyst solution, followed by rinsing and immersion in a monomer solution for 1 h, ellipsometry showed that only  $\sim 2$  Å of material was present, and the F/Si ratio of this sample as determined from XPS analyses was very low. These results confirm that significant film growth is observed only when the substrate is processed sequentially to deposit both the optimal concentration of the anchoring group and the catalyst.

**Surface Polymerization Kinetics.** Representative (ellipsometrically measured) kinetic data for the growth of a polymer film of **5** prepared by ROMP on the 40% **3** primer layer are shown in Figure 7. The data reveal two important facts related to the mechanism. First, the deposition rate is sensitive to the concentration of the monomer. Second, the catalyst deactivates completely over a period of several hours.

The film growth kinetics can be explained by a set of rate equations based on the coupled chemical reactions shown in Figure 8. Several assumptions underlie this analysis. We assume that the surface-tethered ROMP is initiated by the initial number of active catalyst sites per unit area,  $P_i$ , a value that essentially depends on the primer composition. Polymer chains grow by one unit of monomer per step at a propagation rate of  $k_p$  in a second-order reaction, resulting in a polymer consisting of a chain of  $i$  monomers after  $i$  steps. We also assume that, under

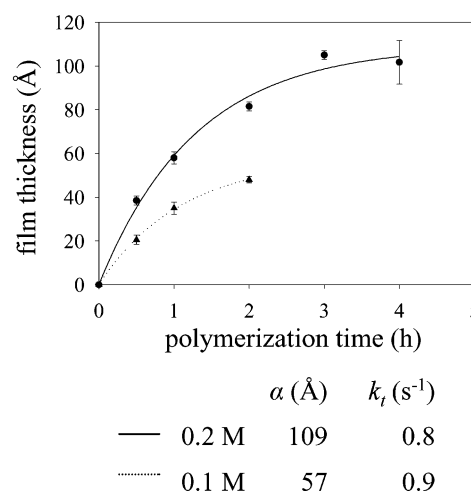


**Figure 7.** Ellipsometric thickness of polymer films recorded as a function of immersion time in the monomer solution of **5** using Si wafers coated with a 40% **3** primer ( $\theta \approx 0.3\theta_{\text{sat}}$ ). The plots were fitted to  $\text{thickness} = \alpha(1 - e^{-k_t t})$ , where  $\alpha = (k_p M m_0 P_i) / (k_t \rho)$ . The values of  $\alpha$  and  $k_t$  are listed below the plots, and the terms are defined in the text.

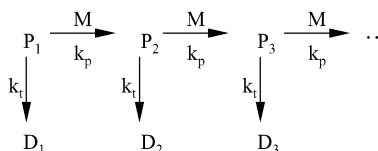


**Figure 8.** Schematic depiction of a surface-confined ROMP process: competitive step growth and termination processes.

the conditions employed in our experiments, the active species in each step are susceptible to deactivation (irreversibly) by a first-order reaction at a rate of  $k_t$ . For simplicity, we assumed that the rate constants  $k_p$  and  $k_t$  are independent of the chain length. We define  $L$  as the total number of polymerized monomer units on the surface per unit area,  $M$  as the concentration of the monomer in solution,  $P_i$  as the number of growing polymer chains of length  $i$  per unit surface area, and  $t$  as the polymerization time. (The symbol  $P_0$  will stand for the time-dependent concentration of active Ru centers that have not yet deactivated or reacted with a monomer; the value of  $P_0$  at  $t = 0$  is  $P_i$ .) We point out that  $M$  is a constant over the course of the polymerization reaction, because the number of monomers that become attached to the surface as polymer is an extremely small fraction of the total number of monomers in solution.

Because the amount of polymer deposited on the surface is proportional to the amount of monomer consumed, the two quantities are related by eq 1:

$$\frac{dL}{dt} = -q \frac{dM}{dt} \quad (1)$$

where  $q$  is a proportionality constant that equates the units of each side of the expression. The total rate of monomer consumption is equal to the sum of the rates of monomer consumption in each propagation step so that, according to the chemical reactions described in Figure 8, the term  $dL/dt$  is defined by eq 2, where the proportionality constant  $q$  has been subsumed into the rate constant  $k_p$ .

$$\frac{dL}{dt} = -(-k_p M P_0 - k_p M P_1 - \dots) = k_p M \sum_{i=0}^{\infty} P_i \quad (2)$$



The concentrations of the propagating chains  $P_i$  are time dependent, and their values must be derived from the rate expressions that govern the reactions of each individual chain. For  $P_0$ , the surface concentration of active Ru centers that have not yet reacted with monomer, the relevant differential equation is:

$$\frac{dP_0}{dt} = -k_p MP_0 - k_t P_0 \quad (3)$$

This equation is easily integrated, subject to the boundary condition that  $P_0 = P_i$  at  $t = 0$ . For the values of  $P_i$  for  $i > 0$ , the change in the concentration of a chain of length  $i$  depends on the concentration of the chain of length  $i - 1$ , so that an expression for the time dependence of  $P_{i-1}$  must be determined before the time dependence of  $P_i$  can be calculated.

$$\frac{dP_i}{dt} = k_p MP_{i-1} - (k_p M + k_t) P_i \quad \text{for } i > 1 \quad (4)$$

Solving these equations involves a bootstrapping sequence: by substituting the expression previously found for  $P_{i-1}$  and then integrating, an expression for the time dependence of the next variable,  $P_i$ , can be found.

$$\begin{aligned} P_0 &= P_i e^{-t(k_p M + k_t)} \\ P_1 &= k_p MP_0 e^{-t(k_p M + k_t)} \\ P_i &= \frac{(k_p M)^{i-1}}{(i-1)!} P_1 t^{i-1} e^{-t(k_p M + k_t)} \end{aligned} \quad (5)$$

Substituting the expressions for  $P_i$  derived above into eq 2 and integrating the result afford an expression (eq 6) for  $L$ , the total amount of polymer per unit area, where  $a = -k_p M - k_t$  and  $b = k_p M$ .

$$\begin{aligned} \int dL &= \\ b \int &\left( P_1 e^{at} + b P_1 t e^{at} + \frac{b^2 P_1 t^2}{2!} e^{at} + \frac{b^3 P_1 t^3}{3!} e^{at} + \dots \right) dt \quad (6) \end{aligned}$$

Integration and simplification of eq 6 leads to the function shown in eq 7 after applying the boundary condition  $L = 0$  at  $t = 0$ .

$$\begin{aligned} L &= b P_1 \int e^{at} \left( 1 + bt + \frac{b^2 t^2}{2!} + \frac{b^3 t^3}{3!} + \dots \right) dt + c \\ &= b P_1 \int e^{at} e^{bt} dt + c \\ L &= \frac{k_p M P_1}{k_t} (1 - e^{-k_t t}) \end{aligned} \quad (7)$$

$L$  is further related to the ellipsometric thickness ( $d$ ) of the film by eq 8

$$d = \frac{L m_0}{\rho} = \left( \frac{k_p M}{k_t} \right) \left( \frac{m_0 P_1}{\rho} \right) (1 - e^{-k_t t}) \quad (8)$$

where  $\rho$  is the density of the polymer and  $m_0$  is the mass of the monomer unit.

The data shown in Figure 7 can be fit well by eq 8. For a monomer concentration of 0.2 M, the values derived from the fit are  $(k_p M/k_t)(m_0 P_1/\rho) = 109 \text{ \AA}$  (the thickness of the film at infinite time) and  $k_t = 2.2 \times 10^{-4} \text{ s}^{-1}$ . A rough estimate for the unitless term  $k_p M/k_t$  (the effective chain

length for  $M = 0.2 \text{ mol/L}$ ) is calculated to be  $\sim 19\text{--}57$  on the basis of the following assumptions. The number of polymer chains bound per square centimeter should be approximately equal to the number of alkenylsilane linkers per unit area (this is equivalent to assuming that all of the linkers react with Ru and that most of the Ru centers give polymer chains.) For linear alkylsiloxanes with 10–18 carbons, the area per RSi is  $\sim 21 \text{ \AA}^2$  at full coverage,<sup>53</sup> but because our primer was a submonolayer of 40% **3**, the area per active species is  $\sim 53\text{--}160 \text{ \AA}^2$  with the lower end corresponding to full coverage and the upper limit corresponding to  $1/3$  coverage. We used  $(220 \text{ g/mol})/N_A$  for  $m_0$ , where  $N_A$  is Avogadro's number, and  $1.19 \text{ g/cm}^3$ , the density of the monomer, as an approximate value for the density of the polymer ( $\rho$ ). The estimate of  $k_p$  obtained from these values lies in the range of  $\sim 2 \times 10^{-2}$  to  $6 \times 10^{-2} \text{ s}^{-1} \text{ M}^{-1}$ , which is an order of magnitude larger than those of  $\sim 2 \times 10^{-3}$  to  $5 \times 10^{-3} \text{ s}^{-1} \text{ M}^{-1}$  reported for bulk reactions using catalyst **1**.<sup>55,56</sup> We should note, though, that the XPS data suggest that the Ru coverage is, in fact, very low and likely so at a level that is far less than the value estimated on the basis of the silane coverage and composition. The comparison with the solution data suggests that the true coverage lies below the level of 1% of a monolayer (based on the silane linker). This suggests that the chain lengths are, in fact, much higher than the estimate given above. This analysis thus seems to suggest that the propagation rate constants for the surface tethered catalyst are appreciably faster than those reported for similar polymerizations carried out in a homogeneous solution. We note that, given the uncertainties associated with this model, additional studies will be required to establish the quantitative aspects of this comparison more completely.

**XPS Determination of Polymer Composition.** XPS analyses (Figure 4) of the thin films prepared by a 1 h polymerization of **5** showed features due to the presence of the expected polymer: notable are the F 1s core level peak at 688 eV and the F(KLL) Auger transition at 833 eV. Intensity for the Ru 3p core level peaks was not detectable after the monomer exposure, despite extensive signal averaging. A high-resolution C 1s core level scan (Figure 4d) showed peaks located at 285.0 (hydrocarbon), 287.6 ( $-\text{OCH}_2\text{CF}_3$ ), 289.3 ( $-\text{COO}-$ ), and 292.9 eV ( $-\text{CF}_3$ ). The relative areas of the last three peaks were in a  $\sim 1:1:1$  ratio, consistent with the molecular structure of the monomer.

**AFM Determination of Polymer Morphology.** Figure 9 shows AFM images collected at various stages of the surface-initiated ROMP process. These samples were obtained by treating Si wafers with a primer consisting of 40% **3** ( $\theta_{\text{tot}} \approx 0.3\theta_{\text{sat}}$ ), then with **1**, and finally with a 0.2 M solution of monomer **5**. As the polymerization time increases, the surface morphology changes from a reticulated pattern consisting of both islands and a highly branched network, to a more highly interconnected network featuring circular holes, which eventually are filled in to give a more uniformly coated surface. The height difference between the polymer ridges and the channels or holes observed in the early stages is  $\sim 70\text{--}80 \text{ \AA}$ ; the film becomes smoother as it reaches the final stages in the growth process, with the maximum height difference decreasing to  $\sim 30\text{--}40 \text{ \AA}$ . As indicated by these AFM images, the film morphology changes dramatically during the course of the polymerization.

(55) Bielawski, C. W.; Grubbs, R. H. *Macromolecules* **2001**, *34*, 8838–8840.

(56) Robson, D. A.; Gibson, V. C.; Davies, R. G.; North, M. *Macromolecules* **1999**, *32*, 6371–6373.

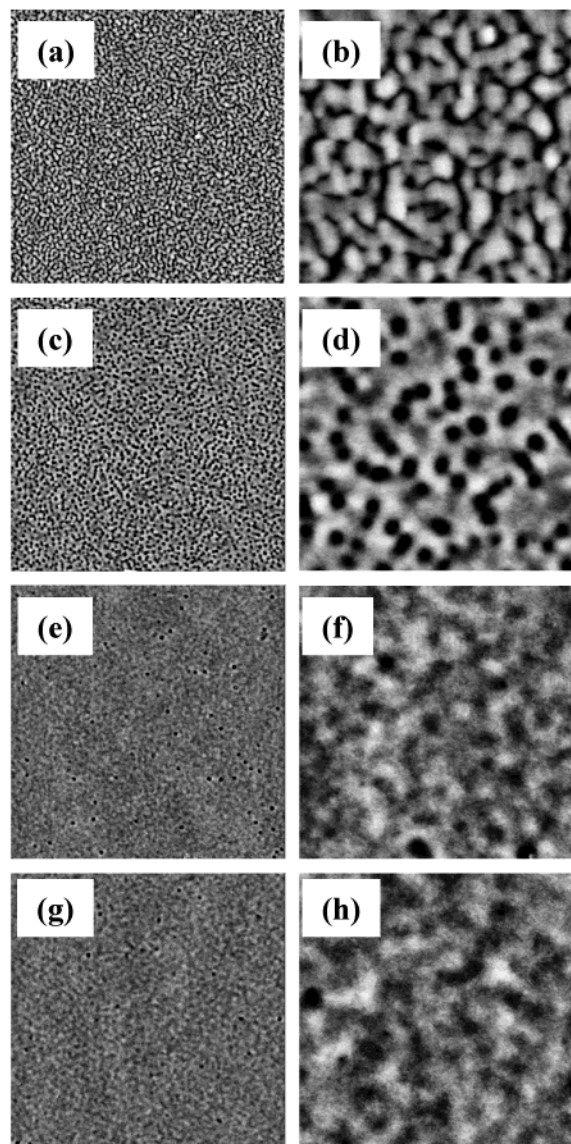


**Figure 9.** AFM images of polymer films prepared from a 0.2 M solution of **5** grown via ROMP on 40% **3** ( $\theta_{\text{tot}} \approx 0.3\theta_{\text{sat}}$ ). The images shown in the right column are high-resolution scans ( $1 \mu\text{m} \times 1 \mu\text{m}$ ) of the images shown in the left column ( $5 \mu\text{m} \times 5 \mu\text{m}$  scans). The ellipsometric thickness and polymerization time are as follows: (a, b)  $\sim 40 \text{ \AA}$ , 30 min; (c, d)  $\sim 60 \text{ \AA}$ , 1 h; (e, f)  $\sim 83 \text{ \AA}$ , 2 h; (g, h)  $\sim 94 \text{ \AA}$ , 4 h. The image contrasts in parts f and h are enhanced for clarity.

The AFM images shown in Figure 10 illustrate the sensitivity of the polymerization process to the catalyst concentration present at the surface and also to the “age” of the Ru catalyst. The two samples shown in Figure 10 were both prepared following the same protocol as the sample shown in Figure 9, parts c and d, but using either new or aged (i.e., a catalyst solution that is allowed to stand for several hours in the absence of a monomer) samples of **1**. The mass coverages and polymer film morphologies differ markedly in these cases, an observation that illustrates the significant experimental sensitivities present in this system of catalytic amplification. Whether for reasons of variability in the Ru catalyst or the linker SAM, systems yielding low limiting mass coverages of the polymer film typically presented islands of various sizes with lower packing densities as compared to thicker, more complete polymer films. The **3**:**4** ratio in the ink and the total mass coverage of the mixed composition primer SAM appear to be the most critical variables,

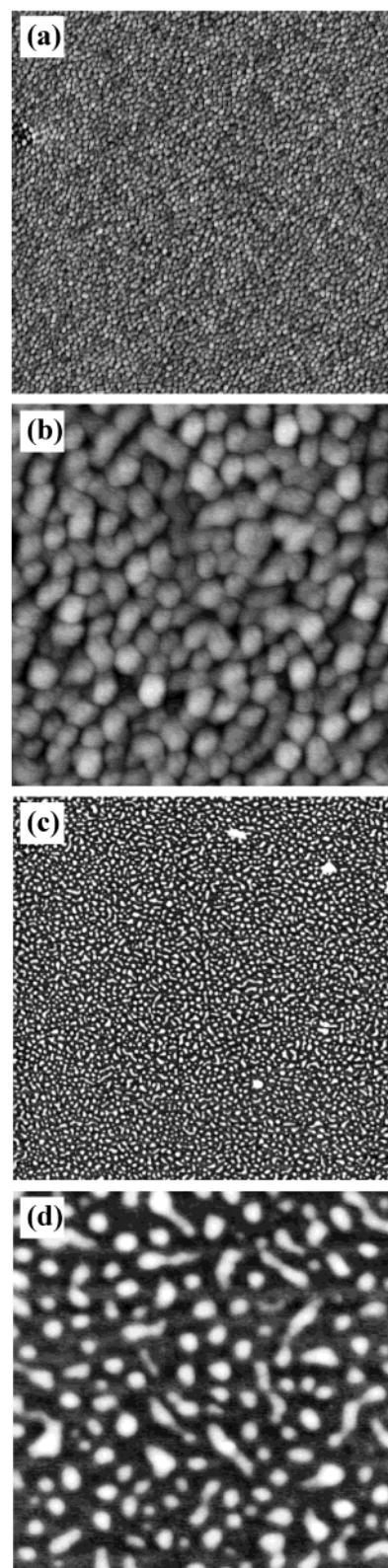


**Figure 10.** AFM images of polymer films prepared from a 0.2 M solution of **5** by ROMP using new (a, b) and aged (c, d) samples of catalyst. The linker used in each case was identical: 40% **3**,  $\theta \approx 0.3\theta_{\text{sat}}$ . The ellipsometric thickness of the films were (a, b)  $\sim 36$  and (c, d)  $\sim 20 \text{ \AA}$ . Images a and c are  $5 \mu\text{m} \times 5 \mu\text{m}$  scans; images b and d,  $1 \mu\text{m} \times 1 \mu\text{m}$  scans.

provided an active sample of the precursor catalyst is used. As noted above, thicker films of polymerized **5** could be obtained by regulating the mole fraction of **3** in the ink in conjunction with the printing contact time.



**Polymerization of Other Strained Olefins.** Although the experimental conditions were not optimized, the polymerization of other strained olefins is also possible on surfaces bearing the mixed primer layer reported here. Norbornene, which is a much more reactive monomer than **5**, gave much thicker films on primed Si wafers, as expected. From a 4 mM solution of norbornene, a  $\sim 230$  Å thick film was obtained in 30 min, using the **3:4** ratio and primer coverage optimized for the ROMP of **5**. The poly(norbornene) film appeared slightly cloudy and non-uniform to the naked eye at this thickness. AFM images of the poly(norbornene) film exhibited isolated islands of various sizes and shapes, many of them larger than those typically observed in films prepared from **5**, and many other large polymer domains.

The optimal fraction of **3** in the primer layer seemed to be higher for norbornene than for **5**, as increasing the amount of **3** in the primer layer resulted in thicker films. The monomer concentration also has a major effect. For example, a poly(norbornene) film deposited by immersing a primed substrate in a 0.1 M norbornene solution for 15 min resulted in film thickness  $\sim 900$  Å; XPS data (Supporting Information) showed that the polymer in this case completely attenuates the substrate core levels at this mass coverage.

Others have reported<sup>38</sup> that Si(111) surfaces derivatized with allyl groups and treated with a Ru ROMP catalyst can promote the growth of poly(norbornene) films of  $9 \pm 1$  Å thickness after 30 min of polymerization using a monomer concentration of 10 mM (cf.  $\sim 230$  Å thick films we obtained from a 4 mM norbornene solution). At a monomer concentration of 90 mM, the reported polymer film thickness ( $120 \pm 14$  Å) is approximately half of what we obtained at 10 mM. The different thicknesses may reflect the amount of **1** present at the surface or the nature of the anchoring groups (three carbon chain vs eight carbon chain), but the exact source of the discrepancy is unclear.

Norbornadiene, another reactive monomer in bulk synthesis, showed little reactivity toward polymerization on the primer layer that was optimized for **5**. The ellipsometric film thickness never exceeded 10 Å; AFM images showed that circular polymer islands 20–50 Å in height were sparsely spread on this latter surface.

The different results obtained for the three different monomers (**5**, norbornene, and norbornadiene) suggest that several termination pathways other than decomposition of the catalyst may be possible in surface-initiated ROMP. First, for high percentages of **3** at the surface, some ring-closing of surface-bound **3** catalyzed by **1** is expected. A likely result of this reaction is a decrease in the surface concentration of **3** and the loss of surface bound Ru sites, but it is unclear how this decrease affects the overall polymer thickness. Second, when two polymer chains are in close proximity to each other, the Ru catalyst bonded to one of the polymer chains may react with an olefin group of the other. Likewise, a surface-bound catalyst may backbite the chain it is attached to. These two cases can lead to cleavage of bound catalysts, and a decrease in the polymer thickness. A third possibility is that termination may occur simply because the growing polymer chains block neighboring active sites. When the polymer chains are separated by a sufficient distance, termination by these mechanisms should be minimized, and a thicker polymer brush obtained.

The amount of the polymer deposited will depend sensitively on the competition between the propagation rate and these termination rates. For example, in the polymerization of relatively unreactive monomers such as **5**, coupling and backbiting of polymer chains (and other

catalyst deactivation processes) compete with growth of polymer chains, thus leading to relatively thin polymer deposits, whereas thicker polymer films will result owing to the faster propagation rates of more reactive monomers such as norbornene. Norbornadiene is a reactive monomer, but because it has multiple sites for reaction, the growth of polymer chains probably competes less effectively in this case with other termination processes.

**Comparison of Different Primer Molecules.** We compared the effectiveness of the linear anchoring group **3** to that of the norbornene-based linker 5-(bicycloheptenyl)trichlorosilane **2** that has previously been used as a primer for surface-initiated ROMP. Using **2** as a linker (which formed a primer layer with a thickness of  $12 \pm 1$  Å after a 24 h immersion in a 60 mM solution of linker) but otherwise following the same protocol as detailed above, the average ellipsometric thickness of the polymer films prepared from **5** was  $59 \pm 13$  Å after 1 h of polymerization. This value is comparable to the thickness obtained when the primer is a mixture of **3** and **4**. XPS data acquired from the polymer films linked to **2** showed an average F/Si ratio of 86/14, which is also similar to the F/Si ratio obtained from the samples prepared on contact printed mixtures of **3** and **4**.

The norbornene-based anchoring agent used in the above experiment was a mixture of endo and exo isomers, whose individual adsorption characteristics on Si/SiO<sub>2</sub> and reactivity toward catalyst binding are unknown, but if both isomers adsorb (as is likely), then the resulting primer layer is a mixed layer just like that formed when the ink is a mixture of **3** and **4**. Furthermore, it is unlikely that **2** forms a well-ordered, dense monolayer on Si/SiO<sub>2</sub>. From this perspective, the active sites generated by a monolayer of **2** may be dilute inherently even without the deliberate addition of unreactive species such as the methyl-terminated **4**. We conclude from these observations that films of equivalent qualities can be produced using cyclic or linear olefin anchors, by adjusting the concentration of the binding functional groups present in the primer layer.

**Patterning via Surface-Initiated ROMP.** Several studies of the patterning of polymer films via surface-initiated polymerization have been reported previously.<sup>18,20,27,31,37,41,57</sup> In most cases, the substrate is patterned by microcontact printing ( $\mu$ CP) with a protective SAM that is used as an orthogonal template, followed by addition of the catalyst and polymerization at the surface.<sup>20,27,31,37,41</sup> We have investigated a similar approach to growing patterned arrays of polymer films (see Figure 1 for our procedure).

We first patterned olefin-free OTS structures by  $\mu$ CP, and then printed the primer (a mixture of **3** and **4**) using an unpatterned stamp. SIMS data from an independent control experiment, in which the **3** present on the surface was brominated with Br<sub>2</sub>, confirmed the orthogonal nature of this two-step directed patterning (Supporting Information): the primer is transferred only in those regions where the OTS SAM is absent.

The resulting patterned surfaces were then treated with Ru catalyst and exposed to monomer **5**. The XPS F 1s core level map taken from a sample coated with the polymer film of **5** is shown in Figure 11. The pattern shown in this figure consists of a square array of circular pixels of  $\sim 150$   $\mu$ m in diameter centered on cross-shaped alignment markers consisting of  $\sim 40$   $\mu$ m  $\times$   $\sim 10$   $\mu$ m lines. The image contrast reveals the orthogonal patterning obtained: the dark area represents the OTS-coating deposited by  $\mu$ CP,

(57) Kratzmüller, T.; Appelhans, D.; Braun, H.-G. *Adv. Mater.* **1999**, *11*, 555–558.

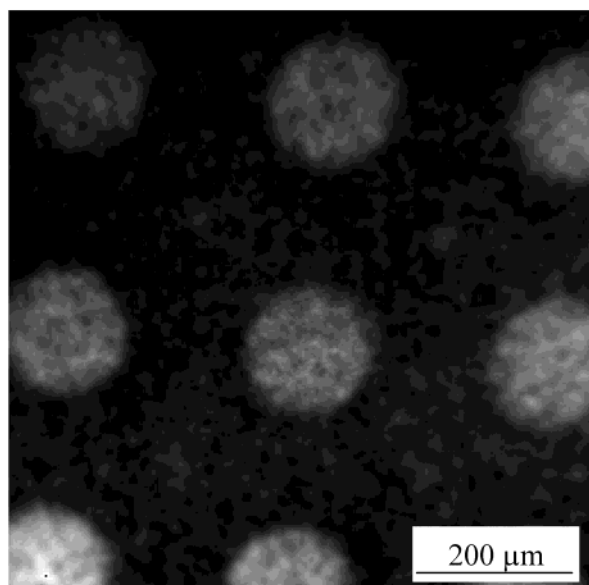


**Figure 11.** XPS F 1s core level image of a patterned polymer sample prepared from a 0.2 M solution of **5**. The circles are  $\sim 150 \mu\text{m}$  in diameter, and alignment markers consist of two intersecting lines of  $\sim 10 \mu\text{m} \times 40 \mu\text{m}$ .

and the bright pixels represent the F atoms of the polymer. The crosses appear rounded in the figure, owing to the low overall photoelectron intensity from these regions and the low resolution of the patterning (see below).

In Figure 12, AFM images of the OTS pattern and the polymer film formed using the OTS template are shown. The printed pattern comprises  $15 \mu\text{m}$  wide lines separated by  $15 \mu\text{m}$  spaces. AFM images of the OTS lines show enhanced height contrast near the line edges, indicating that a higher concentration of OTS multilayers is present in these areas (Figure 12, parts a and b). In addition, detached OTS islands appear near the printed lines, within a  $\sim 2.5 \mu\text{m}$  wide band along the edge of the printed line. Such features have been noted in earlier work.<sup>58</sup> Cross-linked multilayer domains of OTS (bright spots in the AFM images) are also found within the contact printed lines themselves. Although these printing conditions are not optimized for OTS, our goal was simply to form a dense layer of OTS that would not allow penetration of the reagents used in ROMP. The AFM data clearly show that the polymerization of **5** occurred in both the OTS-printed and OTS-free areas of the substrate, as judged from the presence of polymer islands and domains formed throughout the AFM image areas shown in Figure 12, parts c and d. A closer look at the higher magnification view shown in Figure 12d reveals structural differences among the polymer deposits and a gradient in their graft density. The polymer film is more densely grafted in the OTS-free regions of the pattern as evidenced by the large number of reticulated domains. It is striking to note that the polymer of **5** is completely depleted in the regions where OTS multilayers were present as well as those covered by the dense OTS monolayer domains that lay along the line edge (Figure 12, parts b and d). Because the small OTS islands are capable of resisting polymer formation, or adsorption of the primer ink, we believe that OTS can serve as an effective molecular resist when it forms a dense layer. The polymer growth seen in the OTS region, then, must result from defects present in that layer. We believe that the polymer islands seen in the OTS regions are

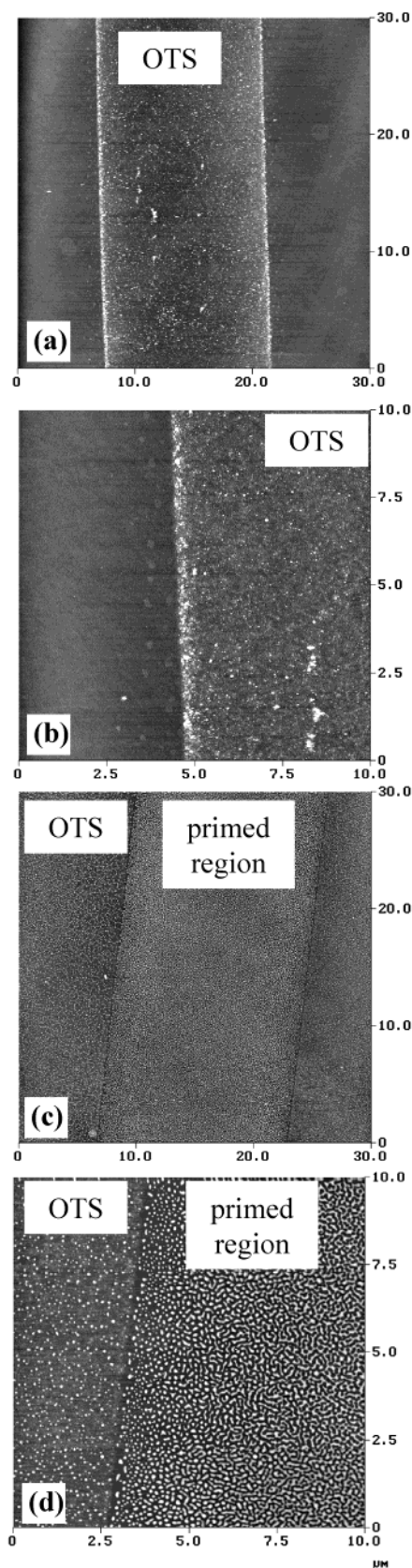


**Figure 12.** AFM images of (a, b) an OTS template formed by  $\mu\text{CP}$  10 mM OTS on a Si wafer and (c, d) polymer film of **5** formed on an OTS template by surface-initiated ROMP. An OTS-patterned wafer was printed with a primer, followed by anchoring of the Ru catalyst and ROMP. The images show printed lines that are  $15 \mu\text{m}$  wide, separated by  $15 \mu\text{m}$  wide spaces. The images in parts a and c are  $30 \mu\text{m} \times 30 \mu\text{m}$  scans, and those in parts b and d are  $10 \mu\text{m} \times 10 \mu\text{m}$  scans.

(58) Jeon, N. L.; Finnie, K.; Branshaw, K.; Nuzzo, R. G. *Langmuir* 1997, 13, 3382–3391.

formed at the intrinsic grain boundaries of the OTS layer and in the defects created by  $\mu$ CP where the small alkene anchoring reagent **3** was able to penetrate and amplify their presence in the passivating layer. As seen in the XPS F 1s core level map recorded at a larger scale (Figure 11), the majority of the ROMP process was confined to the OTS-free areas as directed by the OTS template. Clearly, though, a new strategy for preventing nonselective polymerization from taking place is required and we believe new ink chemistries are needed to improve the quality of the passivating SAM. A more logical solution is to pattern the anchoring reagent directly onto the substrate, without the use of a passivating layer. The ink we chose in this report consists of low molecular weight *n*-alkenyltrichlorosilanes and *n*-alkyltrichlorosilanes, which are not suitable for high-resolution  $\mu$ CP at room temperature. By shifting to a higher molecular weight material with mass-transfer properties suitable for  $\mu$ CP, it should be possible to obtain high-resolution and high-fidelity growth of patterned polymer films. Future work will explore this possibility.

In summary, we demonstrated surface-initiated ROMP of strained olefins using contact printed mixed primer layers of active and inactive components. The initial concentration of the active sites and the reactivity of

monomers showed a profound effect on the polymerization kinetics and the morphology of the resulting polymer films. Although we did not establish optimized protocols for high-resolution patterning directed by microcontact printed OTS passivating layers, the work presented in this report is directly applicable to thin film processing that does not require fine patterning and establishes the mechanistic limitations that result from intrinsic termination reactions of surface-bound catalyst species.

**Acknowledgment.** This work was supported by DARPA (N66001-98-1-8915), the Department of Energy (DEFG02-91ER45439), and the National Science Foundation (CHE-0097096). Surface analyses were carried out at the Center for Microanalysis of Materials, University of Illinois, which is supported by the Department of Energy under Contract DEFG02-91ER45439. We would also like to thank Kari Fossier for her help in the drafting of this manuscript.

**Supporting Information Available:** Figures showing XPS analysis of a poly(norbornene) film deposited on Si(100) and SIMS showing bromination of the double bond. This material is available free of charge via the Internet at <http://pubs.acs.org>.

LA020924V